CircRNA_0000392 Promotes Colorectal Cancer Progression by Sponging miR-193a-5p

Hanchen Xu
Institute of Degistive Diseases, Longhua Hospital, Shanghai University of Tradional Chinese Medicine
https://orcid.org/0000-0003-2335-5421

Yujing Liu
Institute of Degistive Diseases,Longhua Hospital,Shanghai University of Tradional Chinese Medicine

Peiqiu Cheng
Institute of Degistive Diseases, Longhua Hospital, Shanghai University of Tradional Chinese Medicine

Chunyan Wang
Institute of Degistive Diseases, Longhua Hospital, Shanghai University of Tradional Chinese Medicine

Yang Liu
Department of General Surgery,Longhua Hospital, Shanghai University of Tradional Chinese Medicine

Wenjun Zhou
Institute of Degistive Diseases, Longhua Hospital, Shanghai University of Tradional Chinese Medicine

Yangxian Xu
Department of General Surgery, Longhua Hospital, Shanghai University of Tradional Chinese Medicine

Guang Ji (jiliver@vip.sina.com)
Institute of Degistive Diseases, Longhua Hospital, Shanghai University of Tradional Chinese Medicine

---

Research

Keywords: Colorectal cancer, Circular RNAs (circRNAs), RNA-sequencing, circRNA_0000392, miR-193a-5p, PIK3R3

Posted Date: August 20th, 2020

DOI: https://doi.org/10.21203/rs.3.rs-59369/v1

Version of Record: A version of this preprint was published on December 14th, 2020. See the published version at https://doi.org/10.1186/s13046-020-01799-1.

Abstract

Background: Circular RNAs (circRNAs), an important member of the non-coding RNA family, have been revealed the role in the pathogenic progression of diseases in recent years, particularly in the malignant progression of cancer. With the application of high-throughput sequencing technology, a large number of circRNAs have been found in tumor tissues, and some circRNAs have demonstrated the role as oncogenic genes. In this study, we analyzed the circRNA expression profile in colorectal cancer (CRC) tissues and normal adjacent tissues by high-throughput sequencing, focusing on the circRNA_0000392, a circRNA with significantly increased expression in colorectal cancer tissues, and further investigating its function in the progression of colorectal cancer.

Methods: The expression profile of circRNAs in 6 pairs of CRC tissues and normal adjacent tissues was analyzed by RNA-sequencing. We verified the differential circRNAs with expanded samples by qRT-PCR, focused on circRNA_0000392, and evaluated its associations with clinicopathological features. Then we knocked down circRNA_0000392 in CRC cells and evaluated the effect in vitro and in vivo by functional experiments. The dual luciferase assay and RNA pull-down were performed to further explore the downstream potential molecular mechanisms.

Results: CircRNA_0000392 was significantly up-regulated in CRC compared with normal adjacent tissues and cell line. The expression level of circRNA_0000392 was positively correlated with the malignant progression of CRC. Functional studies revealed that reducing the expression of circRNA_0000392 could inhibit the proliferation and invasion of CRC both in vitro and in vivo. Mechanistically, circRNA_0000392 could act as a sponge of miR-193a-5p and regulate the expression of PIK3R3, then affect the activation of the AKT-mTOR pathway in CRC cells.

Conclusions: The circRNA_0000392 has the function as an oncogene through miR-193a-5p/PIK3R3-Akt axis in CRC cells, implying that circRNA_0000392 is a potential therapeutic target for the treatment of colorectal cancer and a predictive marker for CRC patients.

Background

Colorectal cancer (CRC) threatens human health worldwide as the third most common cancers [1]. In recent years, the incidence of colorectal cancer has increased year by year [2]. With the continuous improvement of diagnosis and treatment, the five-year survival rate of colorectal cancer has increased, but the five-year survival prognosis is highly correlated with the stage of the disease. Patients with advanced colorectal cancer were usually accompanied by tumor metastasis, which five-year survival rate was very low [3]. Therefore, it is urgent to further study the pathogenesis of colorectal cancer and the unknown molecular mechanism involved in tumor metastasis.

There is a large amount of non-coding RNA in the human genome, and the relationship between the existence of non-coding RNA and human diseases has always been a research hotspot, especially in malignant tumors. Circular RNAs (circRNAs) is an important member of the non-coding RNA family

following microRNAs and lncRNAs. circRNAs are characterized by the absence of covalently closed loop structures at the 3' and 5' ends. Base on this closed structure, circRNAs are highly stable and not easily degraded [4]. The researchers have discovered the presence of circRNA in multiple organisms such as yeast, mitochondria and eukaryotes and detected more than 20,000 circRNAs in eukaryotes [5, 6]. One study reported that exon rearranged circulating transcripts were first discovered in leukemia cells, Hela cell lines and normal human primary blood cells, and approximately 80 circRNAs were identified [7]. Since then, more and more circRNAs have been identified in different tissues using high-throughput sequencing technology. The role of circRNA in the development of diseases such as encephalopathy and tumors were also gradually revealed [8, 9]. The mechanism of circRNA as a competitive endogenous RNA has become the focus of research on its role in cancers. CircRNA adsorbs miRNA through the sponge action of miRNA to regulate the expression of its target genes [10, 11]. With the continuous expansion of study on circRNAs, circRNAs have been shown to be involved in the development of almost all types of cancers [12–17]. All the studies on the relationship between circRNAs and cancer suggestted that circRNAs may be a novel potential biomarker and therapeutic target. However, since most circRNAs were still exist without exploration and the roles of circRNAs in the CRC progression are still largely unknown, further research is needed to find the circRNAs associated with CRC tumorigenesis and to elucidate their functions.

In this study, we first explored the expression profiles of circRNAs in the 6 paired CRC tissue and adjacent normal tissues by using high-throughput RNA sequencing. A total of 66855 circRNAs were detected, among them, 1687 circRNAs with significant differential expression were identified after CRC tissues was compared with adjacent normal tissues. After verifying some candidate circRNAs by qRT-PCR, we found that circRNA_0000392 was significantly up-regulated in the CRC tissues. The high expression of circRNA_0000392 was associated with the pathological stage and metastasis in CRC. We then focused on circRNA_0000392 and demonstrated that inhibition of its expression could significantly attenuated the proliferation and invasion in CRC cells. More importantly, we explored the mechanism of circRNA_0000392 in the progression of colorectal cancer and found that it could act as a sponge of miR-193a-5p, thereby releasing the inhibition of PIK3R3 by miR-193a-5p and promoting the phosphorylation of AKT / mTOR signaling pathway. Our findings illustrated a new mechanism of CRC progression and provide new insights for its treatment and diagnosis.

Materials And Methods

Patient population and clinical data

The 40 pairs of CRC tissues and adjacent normal tissues were collected from patients who were diagnosed with CRC at the Longhua Hospital affiliated to Shanghai University of Traditional Chinese Medicine (Shanghai, China). Tumor and normal adjacent tissue samples were obtained from the surgical treatment at the Department of General Surgery. The samples were snap frozen in liquid nitrogen after separated from the human body immediately and stored at − 80 °C before using. All the patients have

signed informed consent prior to surgery and did not receive preoperative chemotherapy or radiotherapy. This study was approved by the Ethics Committee of Longhua Hospital.

RNA sequencing, identification and quantification of human circRNAs

The total RNA was isolated from the tissue samples using TRIzol reagent (Life Technologies, Carlsbad, CA) according to the manufacturer's instructions. Then we assessed the RNA integrity and DNA contamination by using electrophoresis on a denaturing agarose gel. After confirming the RNA is intact and pure, we using the Ribo-Zero rRNA Removal Kit (Illumina，San Diego, CA, USA) and the CircRNA Enrichment Kit (Cloud-seq，USA) to remove the rRNA and enrich the circRNAs. The RNA-seq libraries were constructed by using pretreated RNAs with TruSeq Stranded Total RNA Library Prep Kit (Illumina, San Diego, CA, USA) according to the manufacturer's instructions. The libraries were denatured as single-stranded DNA molecules, captured on Illumina flow cells, amplified in situ as clusters and finally sequenced for 150 cycles on Illumina HiSeq™ 4000 Sequencer (Illumina, San Diego, CA, USA，according to the manufacturer's instructions. Paired-end reads were harvested from Illumina HiSeq™ 4000 sequencer, and were quality controlled by Q30. The reads were aligned to the reference genome/transcriptome with STAR software and circRNAs were detected and annotated with DCC software. CircBase database and circ2Trait disease database were used to annotated the identified circRNAs. The differentially expressed circRNAs between the two groups were identified T test statistical methods.

Analyses of circRNA-miRNA-mRNA interaction in CRC

CircRNA-miRNA interaction were predicted by popular target prediction softwares including Circular RNA Interactome and RegRNA. Specific predictions for the target gene of miRNA were based on miRanda, miRDB, miRWalk, RNA22 and Targetscan databases. All the circRNA-miRNA-mRNA networks were constructed by Cytoscape software.

Cell culture

Human CRC cell lines (HT29, HCT116, SW480, SW837, SW48, SW620 and RKO) were purchased from American Type Culture Collection (ATCC) (Manassas, VA, USA). A normal human colon mucosal epithelial cell line (NCM460) and 293 T cell lines were obtained and preserved in our lab. HT29 and HCT116 cells were cultured in McCoy's 5A (Gibco, Carlsbad, CA, USA), SW480, SW620, SW48, SW837 and 293 T cells were cultured in DMEM (Gibco, Carlsbad, CA, USA), NCM460 cells were cultured in M3:10 media (INCELL, San Antonio, TX), and RKO cells were cultured with MEM (Gibco, Carlsbad, CA, USA), all culture medium containing 10% fetal bovine serum and 1% penicillin. All these cell lines were maintained in a humidified atmosphere of 5% CO2 at 37 °C.

Antibodies and reagents

Anti-PIK3R3 antibody (ab97862, 1:1000 dilution for immunoblotting and 1:200 for IHC) was purchased from Abcam. Anti-AKT1 antibody (#2938), anti-phospho-Akt (Ser473) antibody (#4058), anti-mTOR antibody (#2972), anti phospho-mTOR (Ser2448) antibody (#2971) were obtained from Cell Signaling

Technology and all perform a 1:1000 dilution for immunoblotting. The anti-actin (sc-1616, 1:5000 dilution), HRP-anti-mouse IgG (sc-2055, 1:5000 dilution) and HRP-anti-rabbit IgG (sc-2054, 1:5000 dilution) were purchased from Santa Cruz. Actinomycin D and Crystal Violet were purchased from Sigma-Aldrich (St Louis, MO, USA). RNase R was purchased from Epicentre Technologies (Madison, WI, USA).

RNA extraction and qRT-PCR

The total RNA was extracted by using TRIzol reagent (Life Technologies, Carlsbad, CA) and then reverse-transcribed into cDNA using the SuperScript First-Strand Synthesis System (Invitrogen, Carlsbad, CA, USA). The cDNA was used for qPCR using SYBR Green PCR Master Mix (Applied Biosystems, Foster City, CA, USA) with gene-specific primers and the results were normalized with β-actin or U6 as a control. PCR primers are listed in Supplementary Table S1.

circRNA RNase R resistance analysis and actinomycin D assay

The SW620 and RKO cells were treated with 3 U/mg of RNase R (Epicenter, WI, USA) or 2 mg/L actinomycin D (Sigma, USA), then cultured at 37 °C. The cells were harvested at the indicated time points and the stability of circRNA_0000392 and YAF2 mRNA was detected by quantitative real-time PCR (qRT-PCR) assay.

Fluorescence in situ hybridization (FISH)

SW620 and RKO cells were seeded in dishes and fused to 70-80%, then the cells were fixed at room temperature with 4% paraformaldehyde, then treated with protease K. Then overlaid with FITC-labeled circRNA_0000392 probe (Gefanbio, China) at 65 °C for 48h. The signals of the probe were detected by a Fluorescent In Situ Hybridization Kit (Gefanbio, China) according to the manufacturer's protocol. Nuclei were counterstained with DAPI.

Luciferase reporter assay

The sequences of circRNA_0000392 and PIK3R3–3' UTR and their corresponding mutant versions without miR-193a-5p binding sites were synthesized and subcloned into luciferase reporter vector pmirGLO (Promega, Madison, WI, USA), named as circRNA_0000392 -WT, circRNA_0000392-Mut, PIK3R3 3' UTR-WT and PIK3R3 3'UTR-Mut, respectively. The plasmids were validated by sequencing and then co-transfected with the miRNA mimics or inhibitor with the negative controls, respectively. The relative luciferase activity was measured with a Dual Luciferase Assay Kit (Promega, Madison, WI, USA).

Transwell migration and matrigel invasion assays

The transwell chamber (Corning, Kennebunk, ME, USA) was using for the migration assays and the transwell chamber pre-coated with matrigel was using for the invasion assays. According to the protocol, the single cell suspensions were added to the upper chambers and incubated for 24 h. Then wash, fix,

and stain the cells with crystal violet. Base on the crystal violet staining, we calculate the migration and invasion rates through counting cells at least five random fields.

RNA immunoprecipitation (RIP)

RIP assay was performed in SW620 and RKO cells. 1 x 10^7 cells were lysed by RNA lysis buffer completely, then incubated with RIP immunoprecipitation buffer containing magnetic beads conjugated with human anti-Argonaute2 (AGO2) antibody (Millipore, USA) or negative control mouse IgG (Millipore, USA). Add Proteinase K to the sample obtained from RIP and incubate at 55 °C for 30 mins. Then immunoprecipitated RNA was isolated and analyzed by qRT-PCR to quantify the enrichment of circRNA_0000392.

RNA pull-down

Biotin- labeled circRNA_0000392 probe or oligo probe (Gene- Pharma, China) were synthesized. SW620 and RKO cells were lysed with lysis buffer and incubated with specific circRNA_0000392 probes. Then, SW620 and RKO cells were lysed with lysis buffer were lysed in lysis buffer and incubated with probe-coated beads at 4 °C overnight. The beads were washed and the RNA complexes were extracted with TRIzol (Life Technologies, Carlsbad, CA), then detected by qRT-PCR.

Immunohistochemistry

Detection of expression level of PIK3R3 by immunohistochemistry was performed on 5-μm thick paraffin sections based on patient tissue samples. Briefly, the sections were deparaffinized and rehydrated followed by antigen retrieving used 0.01M sodium-citrate buffer (pH 6.0) at a boiling temperature for 10 min. Then let the sections incubated with 3% hydrogen peroxide for 10 min, 5% bovine serum albumin for 1h and primary antibodies at 4 °C overnight. The sections were incubated with secondary antibodies after washing three times with PBS. Finally, the DAB system was used to display colors and the hematoxylin was to stain the nucleus. The immunostaining images were captured using Olympus FSX100 microscope (Olympus, Japan).

Xenograft tumor model

BALB/c nude mice (male 3- to 4-week-old) were injected subcutaneously with 5 × 10^6 SW620 cells. Tumor volumes were measured with a caliper every 3 days, calculated from the length (a) and the width (b) by using the following formula: volume (mm3) = $ab^2/2$. 30 days after injection, the animals were sacrificed, and the excised tumor tissues were removed to further assess tumor weight and pathological staining.

Statistical analysis

Statistical analyses were performed using GraphPad Prism 7.0 (GraphPad Software Inc., CA, USA), The Student's t-test, one-way ANOVA were used to compare differences between groups, as appropriate. The correlation between groups was analyzed by Pearson correlation. ROC curve analysis was performed to

evaluate the diagnostic value. Data were presented as mean ± standard deviation (SD), $p < 0.05$ was considered statistically significant.

Additional methods

Cell transfection, Western blot, Cell proliferation, apoptosis assays are described in Supplementary Methods.

Results

Identification of circular RNAs by RNA-seq analyses in human CRC.

In order to obtain the expression profiles of circRNA and identify differentially expressed circRNAs in CRC patients, the secondary sequencing was used to profile circRNAs expression in paired CRC tissues and adjacent normal tissues (ANT) from 6

patients with CRC. First, the scatter plot was showed the variation of circRNAs expression between the tumor tissues and adjacent normal tissues (Fig. 1A). Then under the cut-off of fold change > 2.0 and $P < 0.05$, the significant differentially expressed circRNAs between the two groups were shown in volcano plot (Fig. 1B) and hierarchical cluster (Fig. 1C). In total, 66855 circRNAs were detected in the tissue samples by the sequencing, among which 19 circRNAs were significant up-regulated while 1668 were significant down-regulated (Fig. 1D and Supplementary Table S2 and S3). GO and KEGG analyses of the host genes of differentially expressed circRNAs were shown in Supplementary Fig. S1 and S2. And base on the source of the circRNA formation, the pie chart showed the percentage of significant differentially expressed circRNAs from intronic, exonic, intergenic, antisense and sense overlapping (Fig. 1E). We then screened out the circRNAs that can be worked as miRNA sponges from the significant differentially expressed circRNAs and constructed a network map using cytoscape software (Supplementary Fig. S3). We overlapped the top 10 circRNAs that are significantly up-regulated or down-regulated (Supplementary Table S4) with circRNAs that function as miRNA sponges. From the overlap, we first selected 4 circRNAs and verified the circRNA-seq results in 40 paired CRC tissues and adjacent normal tissues (ANT) by qRT-PCR. As shown in Fig. 1F, the circRNA_0000392 expression was significantly up-regulated in CRC tissues, which were consistent with the sequencing data. Of the two, circRNA_0000392 has approximately a 25-fold change in sequencing and nearly a 13-fold change in 16 patients, meaning a more significant difference. Therefore, in this study, we will focus on the role of circRNA_0000392 in the tumorigenesis and progression of colorectal cancer.

circRNA_0000392 is up-regulated in CRC and associated with the progression.

To further confirm our results, we increased the number of tissue samples to 40 pairs, and detected the expression level of circRNA_0000392 by qRT-PCR. The results showed that in 29 of the 40 pairs of CRC tissues and adjacent normal tissues, the expression level of circRNA_0000392 was higher in tumor tissues than that of the adjacent normal tissues, and was significantly increased in the overall statistics

of 40 pairs (Fig. 2A and B). Then the ROC curve analysis was performed to assess the diagnostic value of circRNA_0000392 in CRC. It showed that circRNA_0000392 could discriminate CRC from adjacent normal tissues with AUC of 0.713 (95% CI: 0.598 - 0.827, $P < 0.01$) (Fig. 2C). The associations between circRNA_0000392 expression level and clinical parameters of the CRC patients were listed in Table 1. There was no significant difference in the expression level of circRNA_0000392 between the two groups according to age, gender, tumor size and location. But the expression of circRNA_0000392 was significantly correlated with pathological stage ($P = 0.0123$), lymph node metastasis ($P = 0.0055$) and distant metastasis ($P = 0.0084$) (Fig. 2D – G, and Supplementary Fig. S4). The circRNA_0000392 expression level was also measured in a normal human colon mucosal epithelial cell line NCM460 and 7 CRC cell lines including HT29, HCT116, SW480, SW837, SW48, SW620, RKO. It showed that the circRNA_0000392 expression was markedly upregulated in human CRC cell lines compared with normal colon mucosal epithelial cell line (Fig. 2H). These results indicate that the circRNA_0000392 expression was elevated and may be involved in the tumorigenesis and development of CRC.

The characteristics of the circRNA_0000392

Before we delve into its specific role in CRC, we have initially described the characteristics of circRNA_0000392. The genomic loci of circRNA_0000392 was shown in Fig.3A, and the spliced mature sequence length of circRNA_0000392 is 326 bp. Further the SW620 and RKO cells were treated with RNase R exonuclease and actinomycin D to verify the authenticity of circRNA_0000392. The circRNA_0000392 was resistant to RNase R (Fig. 3B) and actinomycin D (Fig. 3C and S4C), while YAF2 mRNA was significantly reduced after RNase R or actinomycin D treatment. RNA fluorescence in situ hybridization (FISH) assay demonstrated that circRNA_0000392 was mainly localized in the cytoplasm (Fig. 3D). These data showed the circRNA_0000392 species was indeed circular.

Knockdown of circRNA_0000392 inhibits CRC cell proliferation and invasion

To explore the function of circRNA_0000392 in CRC cells, we first designed two siRNAs targeting the back-splice region. Then the loss-of-function assays were performed in SW620 and RKO cells with relatively high expression of circRNA_0000392. After transfection the two siRNAs respectively, the expression of circRNA_0000392 was significantly reduced by siRNA #1 in both of the two cell lines (Fig. 4A). WST-1 assay demonstrated that down-regulation of circRNA_0000392 significantly inhibited the proliferation viability of SW620 and RKO cells (Fig. 4B and C). We further analyzed whether circRNA_0000392 has an effect on the cell apoptosis of CRC cells by flow cytometry. By double staining Annexin V and PI, it showed that circRNA_0000392 knockdown significantly enhanced the cell apoptosis at 48 h post-transfection of the siRNA #1 or si-NC (Fig. 4D). Next, the abilities of cell migration and invasion after the siRNA transfection were performed using transwell assays with or without matrigel. As a result, the cell migration and invasion abilities of SW620 and RKO cells were significantly inhibited after knocking down the expression of circRNA_0000392 (Figure. 4E and F). These results indicated that circRNA_0000392 was contributed to CRC cell proliferation and motility in vitro.

circRNA_0000392 functions as a sponge for miR-193a-5p.

It is well known that function as miRNA sponge was one of the important mechanisms by which circRNA exerts its biological functions [10]. Since we previously predicted by prediction software that circRNA_0000392 was one of the circRNAs that could function as miRNA sponges, we mainly focus on the “miRNA sponges” to further explore its underlying mechanism in CRC cell proliferation. First, the RIP assay was performed in SW620 and RKO cells. The results showed that circRNA_0000392 was enriched in AGO2 immunoprecipitates, confirming that the circRNA_0000392 has the miRNA adsorption function (Fig. 5A). Then the circRNA-miRNA-mRNA interaction based on circRNA_0000392 was demonstrated by prediction and bioinformatics analysis using cytoscape software (Fig. 5B). From the prediction, we selected the top 5 candidate miRNAs to validated the specific interaction by RNA pull down assay. The result showed that the miR-193a-5p has a dramatic difference of the pulled down level by circRNA_0000392 probe compared with oligo probe in both SW620 and RKO cells (Figure. 5C and Supplementary Fig. S5A). In order to further confirm the interactions between circRNA_0000392 and miR-193a-5p, the dual- luciferase reporter assay was performed in 293T cells. The circRNA_0000392-wt or circRNA_0000392-mut plasmid was constructed with a luciferase reporter vector (Fig. 5D), and then co-transfected with miR-193a-5p mimic or NC in 293T cells, respectively. The dual-luciferase reporter assay results showed that miR-193a-5p mimics could significantly reduce the luciferase activity of circRNA_0000392-WT group, whereas had no effect on the mutant one (Fig. 5E). The expression levels of miR-193a-5p in 40 pairs of CRC tumor tissues and adjacent normal tissues were measured by qRT-PCR. The results showed that miR-193a-5p expression level in CRC tumor tissues was significantly lower than that in adjacent normal tissues (Fig. 5F and Supplementary Fig. S6). And by Spearman correlation coefficient analysis, there was a negative correlation between miR-193a-5p and circRNA_0000392 expression in CRC tumor tissues (r = -0.365, P =0.021) (Fig. 5G). Overall, these results demonstrated that circRNA_0000392 acts as a sponge for miR-195-5p in the CRC.

PIK3R3 is directly targeted by miR-193a-5p and indirectly regulated by circRNA_0000392.

According to our previous predictions, the EPHA2, PIK3R3, EGFR, USP22 and DDX58 are the most potential target genes for miR-193a-5p. Then we detected the mRNA expression level of these genes after transfected with the miR-193a-5p mimics or inhibitor in SW620 cells. The results revealed that the EPHA2 and PIK3R3 expression level were significantly downregulated by miR-193a-5p mimic and PIK3R3 expression level was upregulated after transfected with the miR-193a-5p inhibitor (Fig. 6A and Supplementary Fig. S7A). The dual-luciferase reporter assay was following performed to confirm the binding relationship between PIK3R3 and miR-193a-5p (Fig. 6B). The PIK3R3 3’UTR WT and mutant plasmid was co-transfected with miR-193a-5p mimic in 293T cells. The results showed that co-transfection of PIK3R3 3'UTR WT plasmid and miR-193a-5p mimic significantly reduced the relative luciferase activity (Fig. 6C). Subsequently, we also tested whether miR-193a-5p affects the expression of PIK3R3. The qRT-PCR results revealed that miR-193a-5p mimic could markedly reduce the expression level of PIK3R3, while the expression level of PIK3R3 could significantly upregulated by miR-193a-5p inhibitor in both SW620 and RKO cell line (Fig. 6D). The protein level of PIK3R3 was significantly down-regulated by the intervention of miR-193a-5p mimic (Fig. 6E). Then we detected the expression levels of PIK3R3 in 40 pairs of CRC tumor tissues and adjacent normal tissues. It showed that the PIK3R3

expression level in CRC tumor tissues was significantly higher than that in adjacent normal tissues and it negative correlated with miR-193a-5p expression in CRC tissues (r = -0.34, *P* =0.032) (Fig. 6F and Supplementary Fig. S7B - D). In order to explore whether the expression level of PIK3R3 could also regulated by circRNA_0000392, we detected the PIK3R3 expression after transfected with circRNA_0000392 siRNA. We found that knockdown of circRNA_0000392 significantly decreased the expressions of PIK3R3 (Fig. 6G). After the IHC staining of PIK3R3 in 40 CRC tissues, we found that PIK3R3 was positively correlated with circRNA_0000392 expression in CRC tissues (r = 0.385, *P* =0.014) (Fig.6H and I). Collectively, these results demonstrated that the PIK3R3 was the target gene of miR-193a-5p and could regulated by circRNA_0000392.

circRNA_0000392 promotes CRC cell proliferation and invasion through circRNA_0000392/miR-193a-5p/PIK3R3 axis.

To investigate whether circRNA_0000392 plays its role in promoting tumor progression through the /miR-193a-5p / PIK3R3 axis, rescue experiments were performed by transcription of miR-193a-5p inhibitors in circRNA_0000392 knockdown cells. The results of WST-1 and transwell assays indicated that the inhibition of proliferation and invasion by circRNA_0000392 knockdown could be rescued by inhibitor of miR-193a-5p in SW620 and RKO cells (Fig.7A - D). And the miR-193a-5p inhibitor could also rescue the effect of circRNA_0000392 knockdown on apoptosis (Supplementary Fig. S8). Then we detected the PIK3R3 mRNA expression by qRT-PCR and found that reduced PIK3R3 expression due to circRNA_0000392 siRNA could be alleviated by miR-193a-5p inhibitor (Fig.7E). In addition, the western blot assay revealed that knockdown of circRNA_0000002 decreased the protein levels of PIK3R3 and the phosphorylation level of AKT and mTOR, then the effects could be reversed by miR-193a-5p inhibitor (Fig.7F - I). Collectively, these results demonstrated that circRNA_0000392 might act as a regulator of miR-193a-5p, which further affects the expression of PIK3R3 to play a regulatory role in CRC.

Downregulation of circRNA_0000392 suppresses the growth of CRC cells in vivo

To explore the effects of circRNA_0000392 in vivo, the circRNA_0000392 knocking down SW620 cells and negative control cells were subcutaneously injected into the back of BALB/c nude mice. After 30 days of observation, the results showed that circRNA_0000392 knockdown reduced the volume and weight of SW620-derived tumors in vivo (Fig.8A - C). Then, the expression levels of Ki-67 and PIK3R3 in the two groups of tumor tissues were evaluated by immunohistochemical staining. As shown in the results, the expression levels of Ki-67 and PIK3R3 were both decreased in the tumor tissues which the expression of circRNA_0000392 was knocked down (Fig.8D - E). Therefore, inhibiting the expression of circRNA_0000392 could significantly inhibit the growth of CRC in vivo (Fig.8F).

Discussion

Colorectal cancer is one of the most common malignant tumors, and its incidence has increased year by year. In terms of treatment, although early CRC can be treated by endoscopic minimally invasive surgery and surgical eradication, since most CRC have no obvious clinical symptoms in the early stage, about

60% of CRC patients develop into the middle and late stages at the time of diagnosis, with lymph node and distant metastases [3]. For colorectal cancer, early detection and treatment can achieve a better prognosis, so it is important to screen for effective new biomarkers and to explore CRC pathogenesis-related signaling pathways.

As a member of non-coding RNA, circRNAs form a closed continuous loop by covalent attachment of 3' RNA and 5' RNA [4, 18]. As early as the 1970s, Sanger et.al [19] discovered the presence of single-stranded circular RNA in plant viruses. However, due to the limitations of detection, circRNA was considered to be a phenomenon of incorrect splicing during exon transcription [20], and thus its existence did not recieved sufficient attention at that period. In recent years, with the development of high-throughput sequencing technology and bioanalysis, circRNA has become a research hotspot in the field of biomedicine [21, 22]. CircRNA is widely expressed in human cells and is tissue-specific, with varying levels of expression in different type of tissues [23]. Due to the characteristics of circRNA, it has become a promising diagnosis a marker or therapeutic target for cancer. To date, many studies have identified circRNAs as diagnostic and prognostic biomarkers in distinct human cancers [24–26], and also reported the role of circRNAs in the progression of cancers [27–30]. However, the expression profile and

In our study, we performed the high-throughput sequencing of circRNA in cancer tissues and adjacent normal tissues of 6 colorectal cancer patients, and obtained the expression profile of circRNA of colorectal cancer containing 66,855 circRNAs. Then the circRNAs differentially expressed in colorectal cancer tissues were identified by bioinformatics analysis. These circRNAs may become potential biomarkers and therapeutic targets for the diagnosis of colorectal cancer. Based on the data we analyzed, we selected some circRNAs with significant differences in expression and validated in extended samples. We found that circRNA_0000392 was significantly upregulated in colorectal cancer tissues and cell lines. And the expression level of circRNA_0000392 in colorectal cancer was markedly associated with clinical stage and malignant progression. The ROC curve analysis showed the diagnostic value of circRNA_0000392 in CRC, revealing that it may be a promising prognostic biomarker. Next, a series of functional experiments demonstrated that knockdown of circRNA_0000392 significantly inhibited cell proliferation and invasion of CRC cells, revealing its function as an oncogene.

In the research on circRNAs to date, the mechanism that could be used as a miRNA sponge has been one of the foundations for exploring its biological functions. Since Hansen [10] discovered that circRNA could function as a miRNA sponge and identified the ciRS-7 with a sponge function of miRNAs, a large amount of circRNAs with miRNA sponge function were revealed in human cancers [15, 31–32]. The RIP assay was used to confirmed that the circRNA_0000392 has the miRNA adsorption function. And based on circRNA_0000392, we first predict circRNA- miRNA- mRNA interactions through target prediction software and constructed the networks. From the predicted candidates, we further confirmed that circRNA_0000392 could directly interact with miR-193a-5p by using RNA pull-down and dual luciferase reporter assays. The results of rescue experiments showed that the effect of decreased CRC cell proliferation and invasion caused by circRNA_0000392 knockdown was offset by inhibition of miR-193a-5p. It has been reported that miR-193a-5p mainly contribute as a tumor suppressor in a variety of cancers

[33–35], and the interaction of circRNA_0000392 with miR-193a-5p attenuated the tumor suppressor efficiency of miR-193a-5p. Our results demonstrated that circRNA_0000392 serves as an oncogene by sponging the miR-193a-5p in CRC.

As a member of non-coding RNA, miRNAs were well known to exert biological effects by modulating their target genes. Those circRNAs with miRNA sponge function could adsorb miRNAs and release the targeted genes of miRNAs indirectly. After we determined that the miR-193a-5p could be adsorbed by circRNA_0000392, our next focus was to search for its effector target genes. Similarly, from the prediction we selected several of the most potential target genes, and by identification, we finally determined the PIK3R3. Our results showed that miR-193a-5p could specifically bind to the 3' UTR region of PIK3R3, and regulated its expression level.

PI3K signaling is widely activated in human cancers and its role in tumor development and metastasis has been well-investigated. PIK3R3 was one of the mammalian gene from Class IA PI3Ks, encode p85a, p85b and p55g regulatory subunits [36]. It has showed that the PIK3R3 regulatory subunit was important for cell proliferation and tumorigenesis [37]. Also, PIK3R3 was overexpressed in some cancers and has been reported as an oncogene. Our data showed that the mRNA and protein expression levels of PIK3R3 in CRC tissues were elevated compared with those in adjacent normal tissues and had a significant positive correlation with the expression level of circRNA_0000392. Studies has showed that the expression level of PIK3R3 in CRC and ovarian cancer tissues has the same trend, which consisted with our results [38, 39]. Our in vitro results showed that while knocking down the expression of circRNA_0000392, it could inhibit the CRC cell proliferation and invasion, while the expression level of PIK3R3 and phosphorylation levels of AKT1 and mTOR were also inhibited. Subsequently, rescue experiments also showed that the miR-193a-5p inhibitor restored the inhibition of cell proliferation by knocking down circRNA_0000392, and also restored the inhibition of this pathway by down-regulation of circRNA_0000392.

Conclusion

In conclusion, we revealed that circRNA_0000392 was upregulated in human CRC tissues by high-throughput sequencing, and it is a promising biomarker for CRC. Furthermore, we first demonstrated that circRNA_0000392 acts as a sponge of miR-193a-5p to regulate the expression of PIK3R3, revealing the effect of the circRNA_0000392/ miR-193a-5p /PIK3R3 axis on the activation of the AKT-mTOR pathway, which is a novel mechanism for CRC progression. This study implied that circRNA_0000392 is a potential therapeutic target for the treatment of colorectal cancer and a predictive marker for CRC patients.

Abbreviations

CRC: Colorectal cancer; circRNA: Circular RNAs; qRT-PCR: Real-time quantitative polymerase chain reaction; IHC: Immunohistochemistry; RIP: RNA immunoprecipitation; ncRNA: Non-coding RNAs; PIK3R3: Phosphoinositide-3-Kinase Regulatory Subunit 3; ROC: Receiver operating characteristic; AUC: Area under

the curve; EPHA2: EPH Receptor A2; EGFR: Epidermal Growth Factor Receptor; USP22: Ubiquitin Specific Peptidase 22; DDX58: DExD/H-Box Helicase 58.

Declarations

Ethics approval and consent to participate

The human cancer tissues used in this study were approved by the institute

ethical committee of Longhua Hospital affiliated to Shanghai University of Traditional Chinese Medicine.

Consent for publication

The consent forms were signed by every participant, and will be provided upon request.

Availability of data and materials

The datasets used during the current study were available from the corresponding authors on reasonable request.

Competing interests

The authors declare that there was no conflict of interest.

Funding

This work was supported by the National Nature Science Foundation of China (No.81874206), Shanghai Rising-Star Program (20QA1409300), Program for Young Eastern Scholar at Shanghai Institutions of Higher Learning.

Authors' contributions

HCX, YXX, and GJ discussed and designed this study; HCX, YJL, PQC and CYW performed the experiments; YL and YXX was responsible for collecting tissue specimen; HCX and WJZ conducted the data analyses; HCX drafted the manuscript. There are two corresponding authors in this manuscript. YXX has contributed to leading the surgery and collecting tissue specimen. GJ has contributed to study design, data interpretation, and editing the manuscript. All authors read and approved the final manuscript.

Acknowledgements

We thank Cloud-Seq Biotech Ltd. Co. (Shanghai, China) for the CircRNA-Seq service.

References

1. Siegel RL, Miller KD, Fedewa SA, Ahnen DJ, Meester RGS, Barzi A, et al. Colorectal cancer statistics, 2017. CA Cancer J Clin. 2017;67:177–93.
2. Siegel R, Fedewa SA, Anderson WF, Miller KD, Ma J, Rosenberg PS, et al. Colorectal cancer incidence patterns in the United States, 1974–2013. J Natl Cancer Inst. 2017;109(8):322.
3. Miller KD, Siegel RL, Lin CC, Mariotto AB, Kramer JL, Rowland JH, et al. Cancer Treatment and Survivorship Statistics, 2016. CA Cancer J Clin. 2016;66:271–89.
4. Memczak S, Jens M, Elefsinioti A, Torti F, Krueger J, Rybak A, et al. Circular RNAs are a large class of animal RNAs with regulatory potency. Nature. 2013;495:333–8.
5. Arnberg AC, Van Ommen GJ, Grivell LA, Van Bruggen EF, Borst P. Some yeast mitochondrial RNAs are circular. Cell. 1980;19(2):313–9.
6. Fan X, Zhang X, Wu X, Guo H, Hu Y, Tang F, et al. Single-cell RNA-seq transcriptome analysis of linear and circular RNAs in mouse preimplantation embryos. Genome Biol. 2015;16:148.
7. Salzman J, Gawad C, Wang PL, Lacayo N, Brown PO. Circular RNAs are the predominant transcript isoform from hundreds of human genes in diverse cell types. Plos one. 2012;7(2):e30733.
8. Lukiw W. Circular RNA (circRNA) in Alzheimer's disease (AD). Front Genet. 2013;4(4):307–8.
9. Bachmayr-Heyda A, Reiner AT, Auer K, Sukhbaatar N, Aust S, Bachleitner-Hofmann T, et al. Correlation of circular RNA abundance with proliferation-exemplified with colorectal and ovarian cancer, idiopathic lung fibrosis, and normal human tissues. Sci Rep. 2015;5(8057):8057–8.
10. Hansen TB, Jensen TI, Clausen BH, Bramsen JB, Finsen B, Damgaard CK, et al. Natural RNA circles function as efficient microRNA sponges. Nature. 2013;495:384–8.
11. Hansen TB, Kjems J, Damgaard CK. Cirular RNA and miR-7 in cancer. Cancer Res. 2013;73(18):5609–12.
12. Zheng Q, Bao C, Guo W, Li S, Chen J, Chen B, et al. Circular RNA profiling reveals an abundant circHIPK3 that regulates cell growth by sponging multiple miRNAs. Nature communications. 2016;7:11215.
13. Li XN, Wang ZJ, Ye CX, Zhao BC, Li ZL, Yang Y. RNA sequencing reveals the expression profiles of circRNA and indicates that circDDX17 acts as a tumor suppressor in colorectal cancer. J Exp Clin Cancer Res. 2018;37:325.
14. Yang R, Xing L, Zheng X, Sun Y, Wang X, Chen. The circRNA circAGFG1 acts as a sponge of miR-195-5p to promote triple-negative breast cancer progression through regulating CCNE1 expression. Mol Cancer. 2019;18:4.
15. Han D, Li J, Wang H, Su X, Hou J, Gu Y, et al. Circular RNA circMTO1 acts as the sponge of microRNA-9 to suppress hepatocellular carcinoma progression. Hepatology. 2017;66:1151–64.
16. Zhong Z, Huang M, Lv M, He Y, Duan C, Zhang L, et al. Circular RNA MYLK as a competing endogenous RNA promotes bladder cancer progression through modulating VEGFA/VEGFR2 signaling pathway. Cancer Lett. 2017;403:305–17.

17. Fang J, Hong H, Xue X, Zhu X, Jiang L, Qin M, et al. A novel circular RNA, circFAT1(e2), inhibits gastric cancer progression by targeting miR-548 g in the cytoplasm and interacting with YBX1 in the nucleus. Cancer Lett. 2019;442:222–32.
18. Geng Y, Jiang J, Wu C. Function and Clinical significance of circRNAs in solid tumors. J Hematol Oncol. 2018;11:98.
19. Sanger HL, Klotz G, Riesner D, Gross HJ, Kleinschmidt AK, et al. Viroids are single-stranded covalently closed circular RNA molecules existing as highly base-paired rod-like structures. Proc Natl Acad Sci USA. 1976;73(11):3852–6.
20. Cocquerelle C, Mascrez B, Hetuin D, Bailleul B. Mis-splicing yields circular RNA molecules. FASEB J. 1993;7(1):155–60.
21. Conn SJ, Pillman KA, Toubia J, Conn VM, Salmanidis M, Phillips CA, et al. The RNA binding protein quaking regulates formation of circRNAs. Cell. 2015;160(6):1125–34.
22. Rybak-Wolf A, Stottmeister C, Glazar P, Jens M, Pino N, Giusti S, et al. Circular RNAs in the mammalian brain are highly abundant, conserved, and dynamically expressed. Mol Cell. 2015;58:870–85.
23. Jeck WR, Sorrentino JA, Wang K, Slevin MK, Burd CE, Liu J, et al. Circular RNAs are abundant, conserved, andassociated with ALU repeats. RNA. 2013;19:141–57.
24. Li P, Chen H, Chen S, Mo X, Li T, Xiao B, et al. Circular RNA 0000096 affects cell growth and migration in gastric cancer. Br J Cancer. 2017;116:626–33.
25. Zhang S, Zeng X, Ding T, Guo L, Li Y, Ou S, et al. Microarray profile of circular RNAs identifies hsa_circ_0014130 as a new circular RNA biomarker in non-small cell lung cancer. Sci Rep. 2018;8(1):2878.
26. Chen J, Li Y, Zheng Q, Bao C, He J, Chen B, et al. Circular RNA profile identifies circPVT1 as a proliferative factor and prognostic marker in gastric cancer. Cancer Lett. 2017;388:208–19.
27. Wang R, Zhang S, Chen X, Li N, Li J, Jia R, et al. CircNT5E acts as a sponge of miR-422a to promote glioblastoma tumorigenesis. Cancer Res. 2018;78:4812–25.
28. Yu J, Xu QG, Wang ZG, Yang Y, Zhang L, Ma JZ, et al. Circular RNA cSMARCA5 inhibits growth and metastasis in hepatocellular carcinoma. J Hepatol. 2018;68:1214–27.
29. Liu H, Bi J, Dong W, Yang M, Shi J, Jiang N, et al. Invasion-related circular RNA circFNDC3B inhibits bladder cancer progression through the miR-1178-3p/G3BP2/SRC/FAK axis. Mol Cancer. 2018;17:161.
30. Zhang J, Liu H, Hou L, Wang G, Zhang R, Huang Y, et al. Circular RNA_ LARP4 inhibits cell proliferation and invasion of gastric cancer by sponging miR-424-5p and regulating LATS1 expression. Mol Cancer. 2017;16:151.
31. Chen X, Chen RX, Wei WS, Li YH, Feng ZH, Tan L, et al. PRMT5 Circular RNA Promotes Metastasis of Urothelial Carcinoma of the Bladder through Sponging miR-30c to Induce Epithelial–Mesenchymal Transition. Clin Cancer Res. 2018;24(24):6319–30.

32. Wu Y, Xie Z, Chen J, Chen J, Ni W, Ma Y, et al. Circular RNA circTADA2A promotes osteosarcoma progression and metastasis by sponging miR-203a-3p and regulating CREB3 expression. Mol Cancer. 2019;18:73.
33. Tsai KW, Leung CM, Lo YH, Chen TW, Chan WC, Yu SY, et al. Arm Selection Preference of MicroRNA-193a Varies in Breast Cancer. Sci Rep. 2016;6:28176.
34. Zhou J, Duan H, Xie Y, Ning Y, Zhang X, Hui N, et al. MiR-193a-5p Targets the Coding Region of AP-2a mRNA and Induces Cisplatin Resistance in Bladder Cancers. J Cancer. 2016;7(12):1740–6.
35. Pu Y, Zhao F, Cai W, Meng X, Li Y, Cai S. MiR-193a-3p and miR-193a-5p suppress the metastasis of human osteosarcoma cells by down-regulating Rab27B and SRR, respectively. Clin Exp Metastasis. 2016;33:359–72.
36. Backer JM. The Regulation of class IA PI 3-kinases by inter-subunit interactions. Curr Top Microbiol Immunol. 2011;346:87–114.
37. Hu J, Xia X, Cheng A, Wang G, Luo X, Reed MF, et al. Apeptide inhibitor derived from p55PIK phosphatidylinositol 3-kinase regulatory subunit: a novel cancer therapy. Mol Cancer Ther. 2008;7:3719–28.
38. Wang G, Yang X, Li C, Cao X, Luo X, Hu J. PIK3R3 Induces Epithelial-to-Mesenchymal Transition and Promotes Metastasis in Colorectal Cancer. Mol Cancer Ther. 2014;13(7):1837–47.
39. Zhang L, Huang J, Yang N, Greshock J, Liang S, Hasegawa K, et al. Integrative genomic analysis of phosphatidylinositol 30-kinase family identifies PIK3R3 as a potential therapeutic target in epithelial ovarian cancer. Clin Cancer Res. 2007;13:5314–21.

Tables

Table 1. Associations between circRNA_0000392 levels and clinical parameters in colorectal cancer patients (n = 40)

Characteristic	No. of Patients (%)	circRNA-0000392 expression (2-ΔCt Mean ± SD)	*P* value
Age (y)	40 (100)		
≥60	31 (77.5)	5.458±5.084	0.3699
60	9 (22.5)	7.247±5.645	
Sex	40 (100)		
Men	27 (67.5)	5.497±5.337	0.5310
Women	13 (32.5)	6.615±5.010	
Tumor size (cm)	40 (100)		
≥5	18 (45)	5.839±4.716	0.9810
5	22 (55)	5.879±5.668	
Tumour location	40 (100)		
Left hemicolon	34 (85)	5.365±4.880	0.1536
Right hemicolon	6 (15)	8.668±6.497	
pTNM stage	40 (100)		
-	20 (50)	4.071±3.144	0.0123*
-	20 (50)	7.679±6.294	
Lymph node metastasis	40 (100)		
pN negative	21 (52.5)	3.756±3.416.	0.0055**
pN positive	19 (47.5)	8.218±5.957	
Distant metastasis	40 (100)		
pM negative	34 (85)	4.981±3.995	0.0084**
pM positive	6 (15)	10.940±8.520	

* $P<0.05$; ** $P<0.01$.

Figures

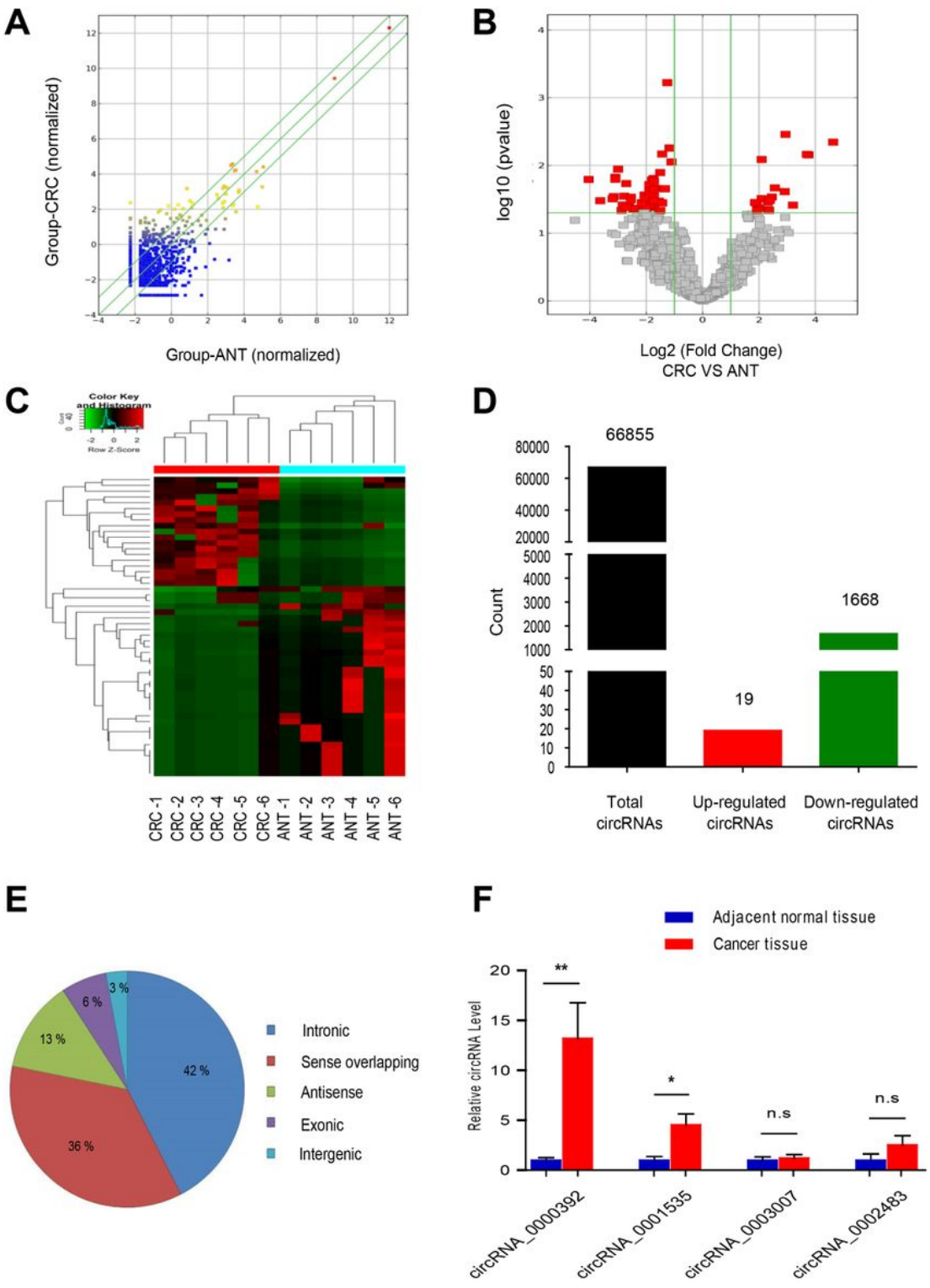

Figure 1

Identification of circular RNAs by RNA-seq analyses in human CRC. (A) The scatter plot figuratively expressed the changes of circRNA expression in six paired CRC and adjacent normal tissues (ANT). CircRNAs above the top green line and below the bottom green line demonstrated more than a 1.5-fold change between the two compared groups. (B) The volcano plot showed the expression profiling of circRNA between the CRC and ANT. The vertical green lines refer to a 2.0-fold (log2 scaled) up-regulation

and down-regulation, respectively. The horizontal green line corresponds to a P-value of 0.05 (-log10 scaled). The red points in the plot represent differentially expressed circRNAs with statistical significance. (C) Clustered heat map indicated differences in circRNA expression profiling between the CRC and ANT tissues. (D) The amount of the total circRNAs by RNA-seq and differentially expressed circRNAs. (E) CircRNAs were classified by category. (F) The validation of the top 4 differential expression circRNAs in 16 paired CRC and ANT tissues by RT-qPCR. CRC, colorectal cancer; ANT, adjacent normal tissue. Data represent mean ± SD. * P < 0.05, ** P < 0.01.

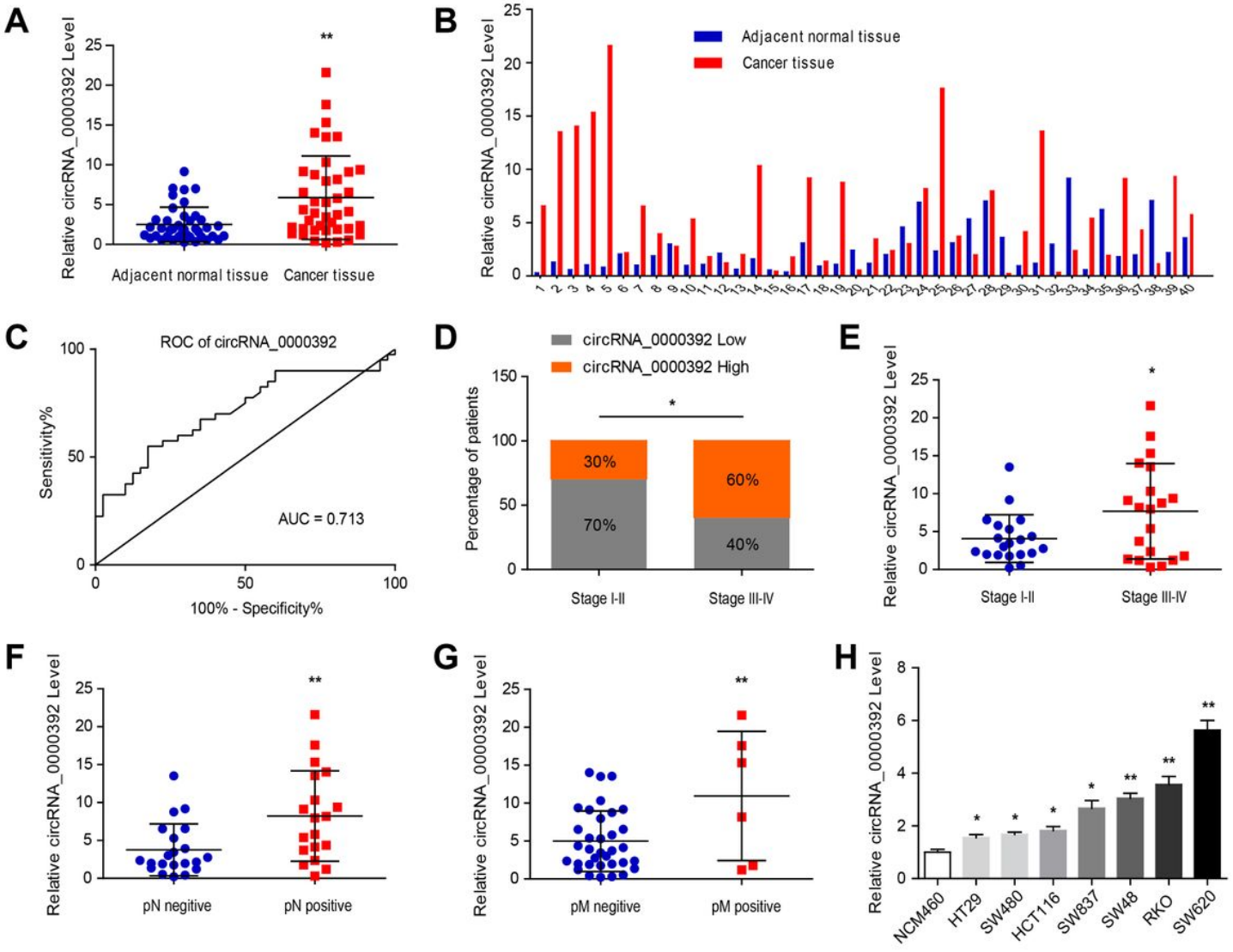

Figure 2

circRNA¬_0000392 is up-regulated in CRC and associated with the progression. (A - B) Relative expression of circRNA_0000392 in 40 pairs of CRC and ANT tissues measured by qRT-PCR. (C) ROC curve analysis of circRNA_0000392 in CRC patients. AUC values are given on the graphs. (D) Percentages of CRC tissues with low or high expression of circRNA_0000392 according to TNM stage. (E) Analysis of circRNA_0000392 expression in CRC patients according to TNM stage. (F) Analysis of circRNA_0000392 expression in CRC patients with or without lymph node metastasis. (G) Analysis of circRNA_0000392

expression in CRC patients with or without distant metastasis. (H) Relative expression of circRNA_0000392 in cell lines was detected by qRT-PCR. Data represent mean ± SD. * P < 0.05, ** P < 0.01.

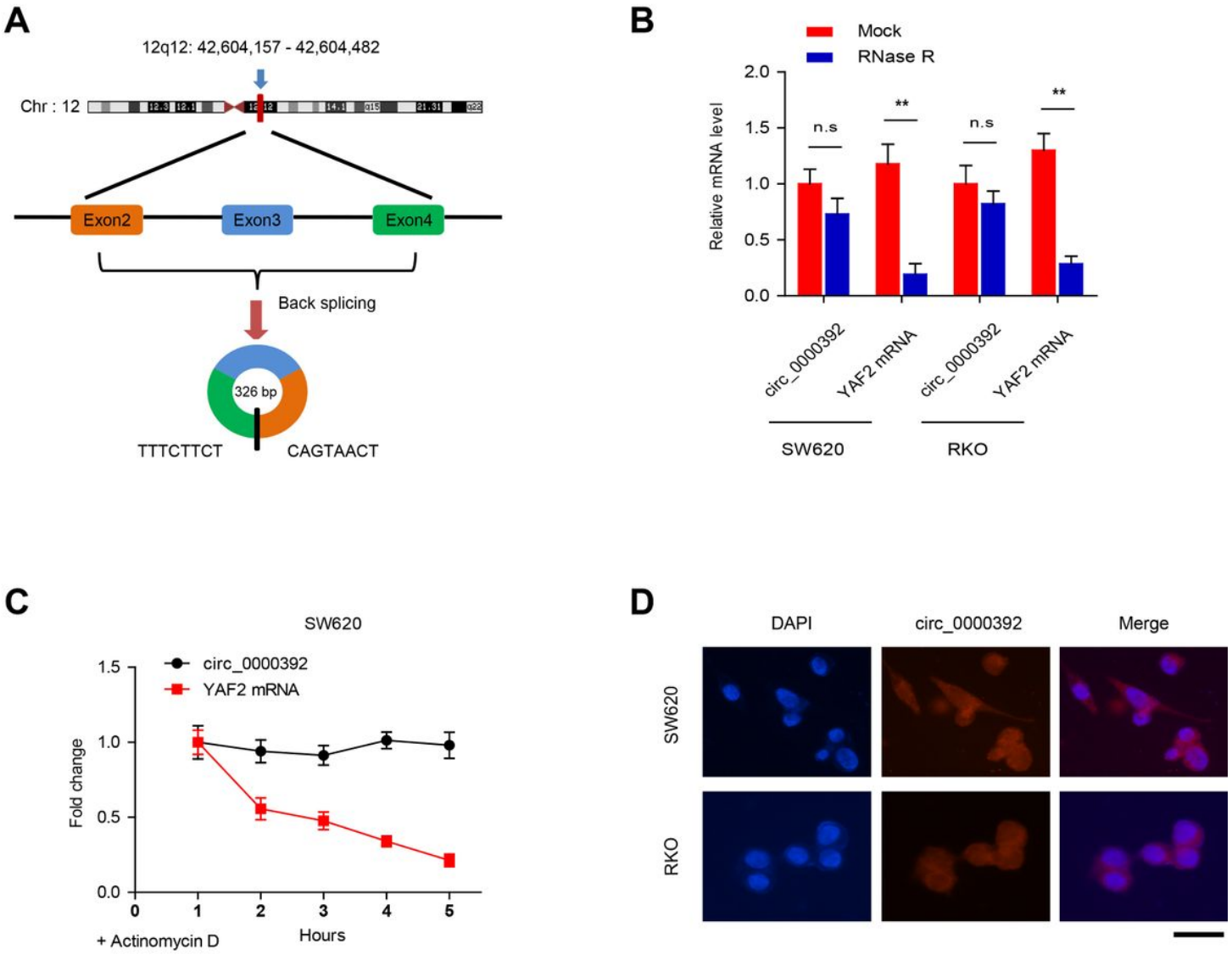

Figure 3

The characteristics of the circRNA¬_0000392. (A) The genomic loci of YAF2 gene and circRNA_0000392. The spliced mature sequence length of circRNA¬_0000392 is 326 bp. (B) The expression of circRNA_0000392 and YAF2 mRNA in SW620 and RKO cells treated with or without RNase R was detected by qRT-PCR. (C) qRT-PCR analysis of circRNA_0000392 and YAF2 mRNA in SW620 cells treated with actinomycin D at the indicated time points. (D) Fluorescence in situ hybridization (FISH) assay was performed to determine the localization of circRNA_0000392 in SW620 and RKO cells. Scale bar = 50 um. Data represent mean ± SD. * P < 0.05, ** P < 0.01.

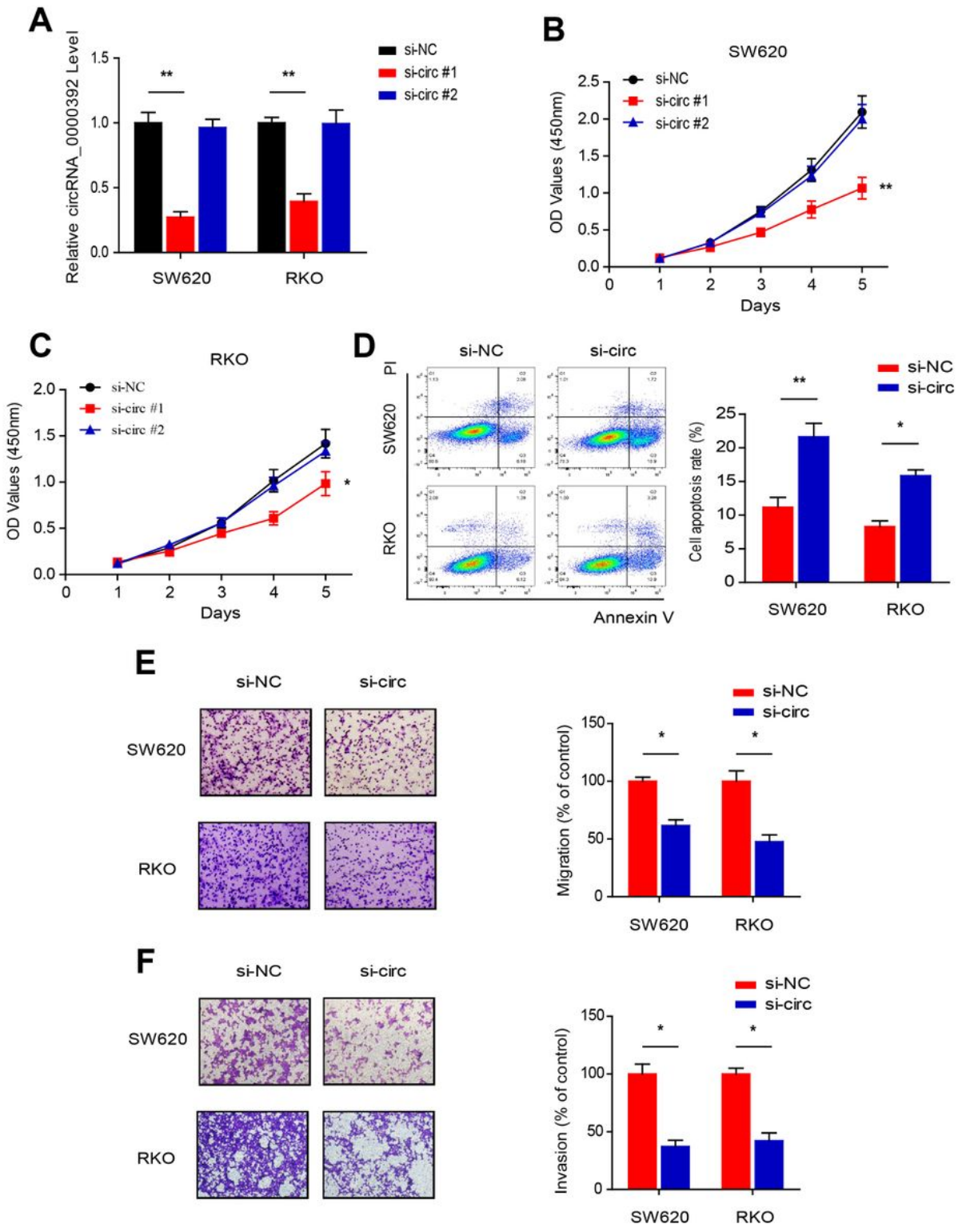

Figure 4

Knockdown of circRNA¬_0000392 inhibits CRC cell proliferation and invasion. (A) qRT-PCR analysis of circRNA¬_0000392 in SW620 and RKO cells after transfection with siRNA. (B - C) The proliferation of SW620 and RKO cells after circRNA¬_0000392 knocking down by siRNA was detected by WST-1 assay. (D) Apoptosis rate was analyzed by flow cytometry after downregulation of circRNA¬_0000392 in SW620 and RKO cells. (E - F) The cell migration (E) and invasion (F) capabilities were assessed by transwell

assay with or without matrigel after circRNA¬_0000392 knocking down in SW620 and RKO cells. Data represent mean ± SD. * P < 0.05, ** P < 0.01.

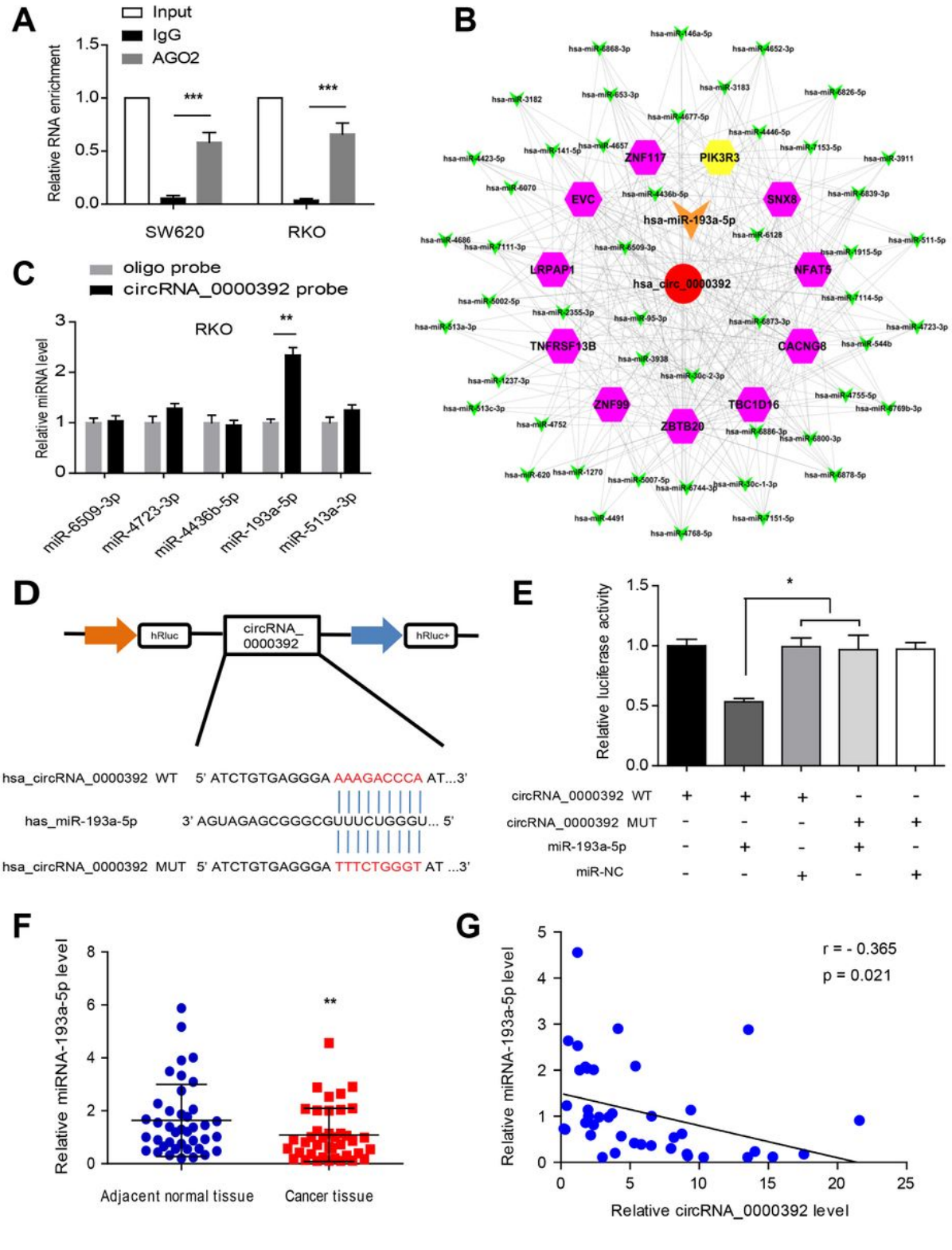

Figure 5

circRNA¬_0000392 functions as a sponge for miR-193a-5p. (A) RIP analysis of circRNA-_0000392 using anti-AGO2 antibody in SW620 and RKO cells. (B) CircRNA-miRNA-mRNA interaction based on circRNA_0000392 was demonstrated by prediction and bioinformatics analysis using cytoscape

software. (C) The top five miRNAs may regulate by circRNA_0000392 base on the miRNA prediction and bioinformatics analyses were showed and measured by qRT-PCR after the pull – down assay in RKO cells. (D) Schematic illustration demonstrates the luciferase reporter vectors containing wild-type (WT) or mutant (MUT) predicted miR-193a-5p binding sites of circRNA_0000392. (E) The luciferase assay was performed in 293T cells after co-transfected with miR-193a-5p mimic and the luciferase vector containing wild-type (WT) or mutant (MUT) circRNA_0000392. (F) Relative expression of miR-193a-5p in 40 pairs of CRC and ANT tissues measured by qRT-PCR. (G) The correlation between circRNA_0000392 and miR-193a-5p in CRC tissues was analyzed by Spearman correlation coefficients. Data represent mean ± SD. * P < 0.05, ** P < 0.01, *** P < 0.001.

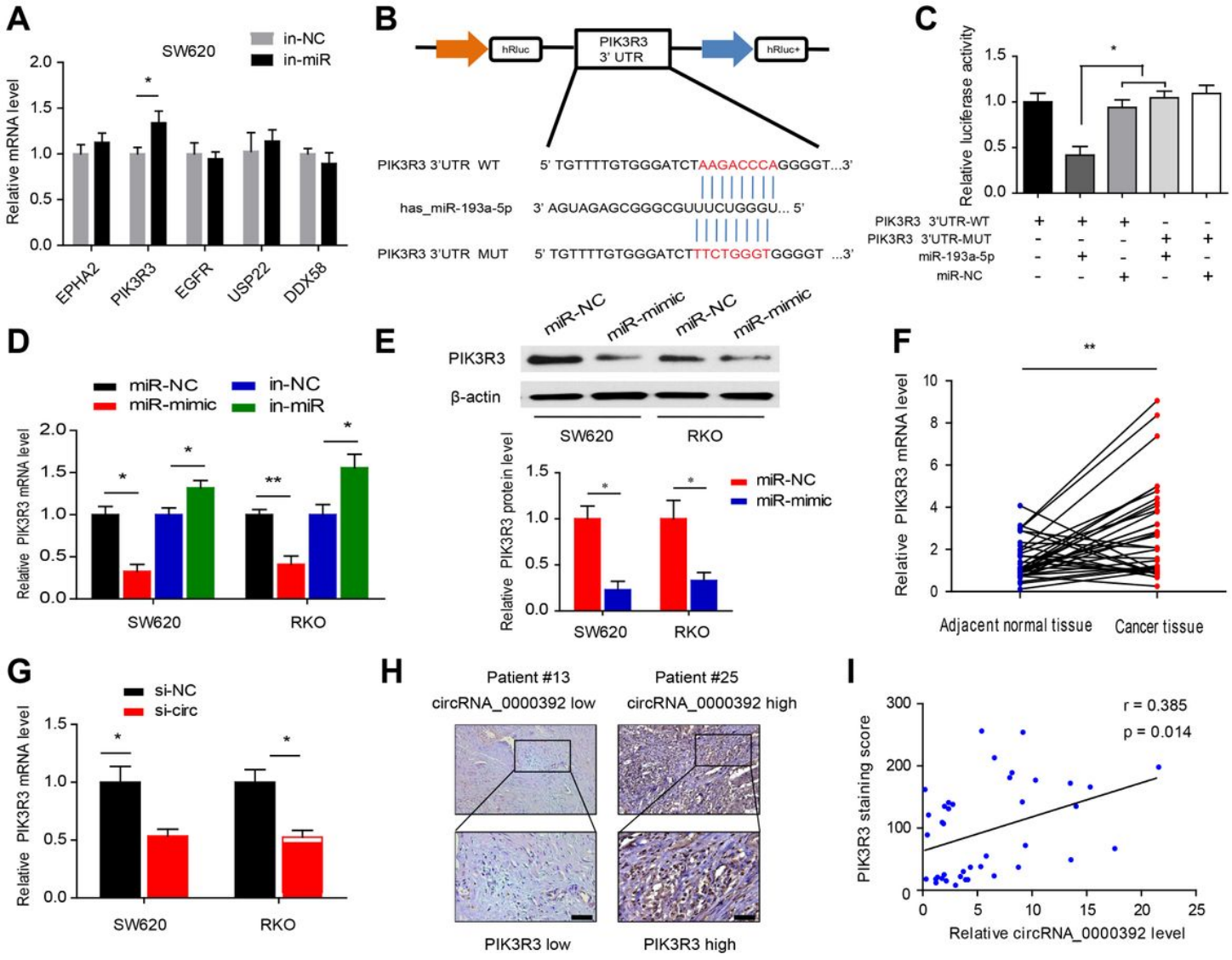

Figure 6

PIK3R3 is directly targeted by miR-193a-5p and indirectly regulated by circRNA¬_0000392. (A) The relative mRNA expression of EPHA2, PIK3R3, EGFR, USP22 and DDX58 after transfected with the miR-193a-5p inhibitor was detected in SW620 cells by qRT-PCR. (B) Schematic illustration of PIK3R3 3'UTR wild-type (WT) or 3'UTR mutant (MUT) luciferase reporter vectors and the predicted binding sites to miR-

193a-5p. (C) The relative luciferase activities were detected in 293T cells after co-transfected with the PIK3R3 3’UTR wild-type (WT) or 3’UTR mutant (MUT) luciferase reporter vectors with the miR-193a-5p mimics. (D) The relative PIK3R3 mRNA expression after transfected with the miR-193a-5p mimics or inhibitor was detected in cells by qRT-PCR. (E) The relative PIK3R3 protein level after transfected with the miR-193a-5p mimics was detected in cells by western blot. (F) Relative expression of PIK3R3 in 40 pairs of CRC and ANT tissues measured by qRT-PCR. (G) The relative PIK3R3 mRNA expression after transfected with circRNA¬_0000392 siRNA was detected by qRT-PCR. (H) Representative IHC staining images of low and high PIK3R3 expression in patient CRC tissue samples. Scale bar = 20 um. (I) The correlation between circRNA_0000392 and PIK3R3 protein expression in CRC tissues was analyzed by Spearman correlation coefficients. Data represent mean ± SD. * $P < 0.05$, ** $P < 0.01$.

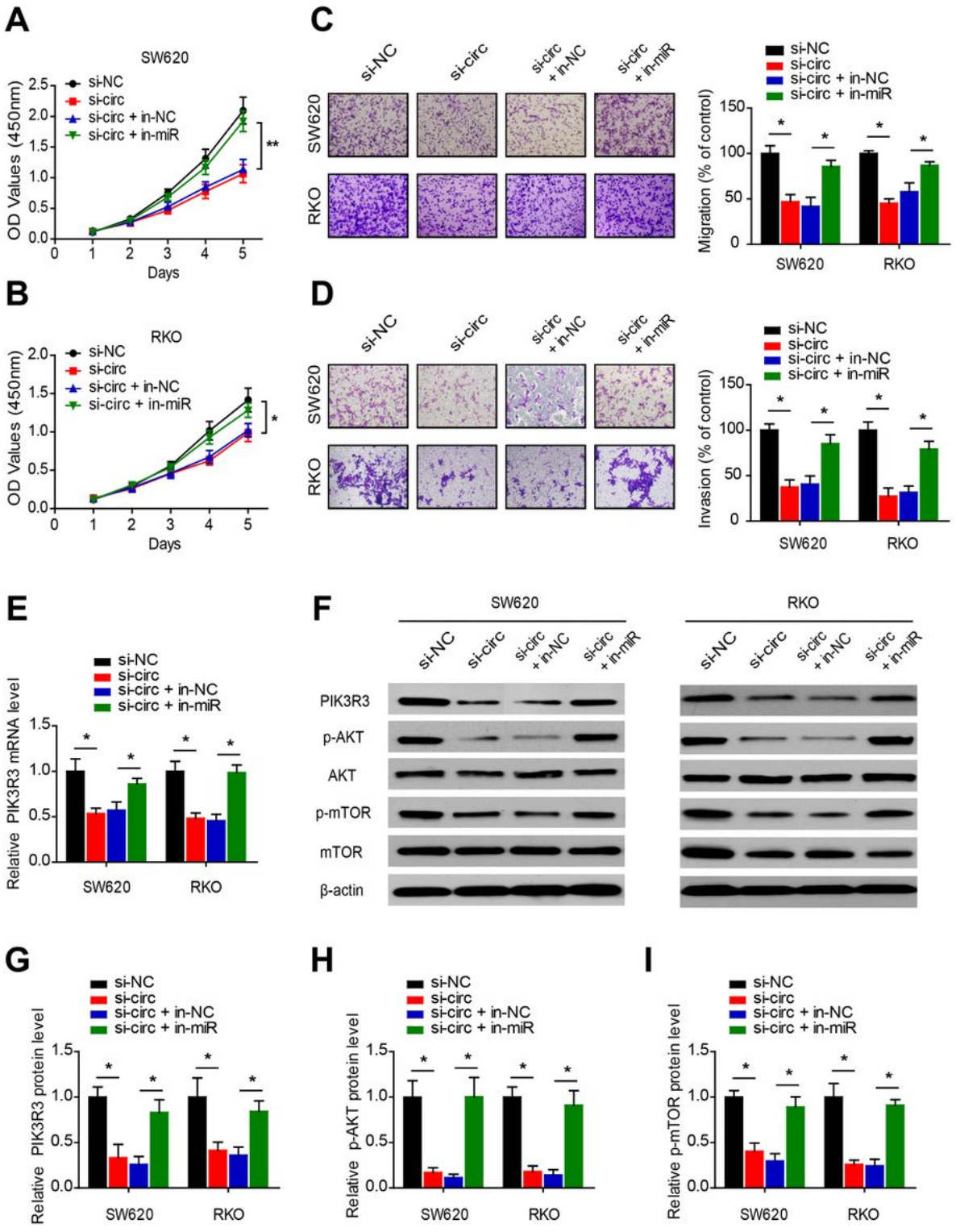

Figure 7

circRNA¬_0000392 promotes cell proliferation and invasion through circRNA_0000392/miR-193a-5p/PIK3R3 axis. (A - B) The proliferation of SW620 and RKO cells after transfected with the circRNA¬_0000392 siRNA and /or miR-193a-5p inhibitor was measured by WST-1. (C - D) The cell migration (C) and invasion (D) capabilities were determined by transwell assay after transfected with the circRNA¬_0000392 siRNA and /or miR-193a-5p inhibitor in SW620 and RKO cells. (E) The relative mRNA

expression of PIK3R3 after transfected with the circRNA¬_0000392 siRNA and /or miR-193a-5p inhibitor was detected by qRT-PCR. (F - I) The relative protein expression of PIK3R3 and the phosphorylation level of downstream pathway proteins were measured by western blot in cells transfected with the circRNA¬_0000392 siRNA and /or miR-193a-5p inhibitor. Data represent mean ± SD. * P < 0.05, ** P < 0.01.

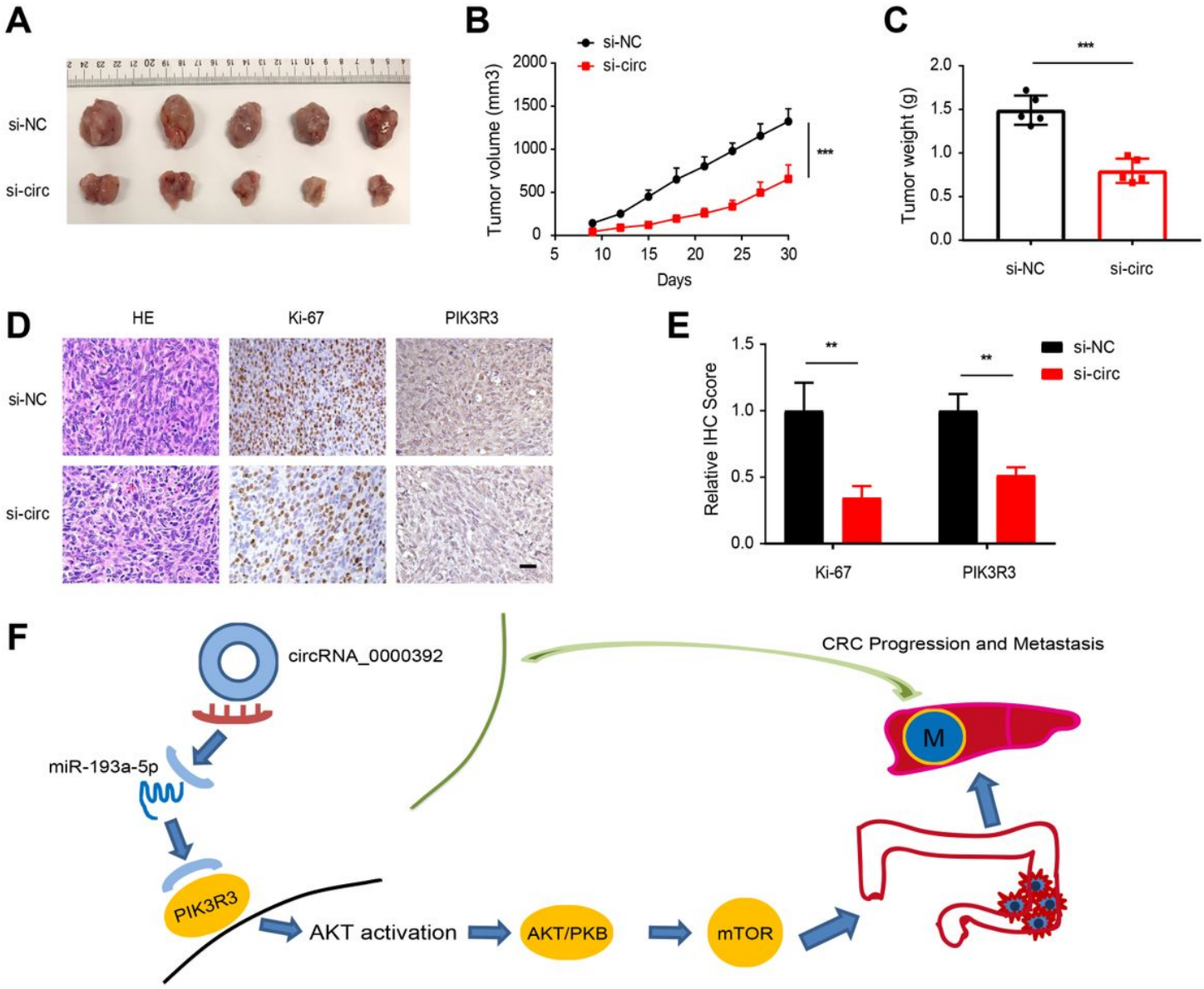

Figure 8

Downregulation of circRNA¬_0000392 suppresses the growth of CRC cells in vivo. (A) Image of subcutaneous xenograft tumors. Nude mice were injected with 5 × 106 SW620 cells (n = 5 for each group). The tumors were extracted after 30 days. (B) Analysis of tumor volume of mice measured every 3 days. (C) Tumor weight in each group at the end of the experiment. (D) Histological analysis of tumor tissues by hematoxylin and eosin staining. IHC of Ki-67 and PIK3R3 in the subcutaneous tumors. Scale bar,100μm. (E) The graph shows relative signal intensity scores of KI-67 and PIK3R3. (F) Schematic

illustration of circRNA¬_0000392 regulating miR-193a-5p/PIK3R3 axis in CRC. Data represent mean ± SD. * P < 0.05, ** P < 0.01, *** P < 0.001.

Supplementary Files

This is a list of supplementary files associated with this preprint. Click to download.

- renamed64ef8.xlsx
- renamedc2962.xlsx
- Additionalfile1.docx